



SYNTHESIS, STRUCTURE AND REACTIVITY OF MONONUCLEAR PARAMAGNETIC COMPLEXES OF ZIRCONIUM AND HAFNIUM

MICHAEL D. FRYZUK* and MURUGESAPILLAI MYLVAGANAM

Department of Chemistry, University of British Columbia, 2036 Main Mall,
Vancouver, B. C. Canada V6T 1Z1

and

MICHAEL J. ZAWOROTKO and LEONARD R. MacGILLIVRAY

Department of Chemistry, St Mary's University, Halifax, N. S. Canada B3H 3C3

(Received 23 March 1995; accepted 8 June 1995)

Abstract—The reduction of the zirconium(IV) precursor $Zr(\eta^5-C_5H_5)Cl_2[N(SiMe_2CH_2PPr^i_2)_2]$ with sodium-amalgam under argon or vacuum generates the mononuclear Zr^{III} complex $Zr(\eta^5-C_5H_5)Cl[N(SiMe_2CH_2PPr^i_2)_2]$ as a thermally stable, crystalline material. Further functionalization of the remaining chloride is possible by the addition of a variety of organometallic reagents, as well as heteroatom nucleophiles. Thus, the hydrocarbyl complexes $Zr(\eta^5-C_5H_5)R[N(SiMe_2CH_2PPr^i_2)_2]$ ($R = Ph, Me, Et, CH_2Ph$ and CH_2SiMe_3) were prepared as well as the heteroatom derivatives $Zr(\eta^5-C_5H_5)X[N(SiMe_2CH_2PPr^i_2)_2]$ ($X = OPh, NPh_2$ and PPh_2); all of the hydrocarbyl and heteroatom substituted Zr^{III} derivatives are mononuclear and were characterized by ESR spectroscopy. In addition, the hafnium(III) complex $Hf(\eta^5-C_5H_5)Cl[N(SiMe_2CH_2PPr^i_2)_2]$ could be isolated via the same procedure but in this case, one could observe the analogous Zr^{III} complex as an impurity. Oxidation of the Zr^{III} and Hf^{III} complexes could be effected by the addition of $TiCl_3$, $PbCl_2$ or $PhSSPh$. Two crystal structures are also included: $Zr(\eta^5-C_5H_5)Ph[N(SiMe_2CH_2PPr^i_2)_2]$ and $Zr(\eta^5-C_5H_5)CH_2SiMe_3[N(SiMe_2CH_2PPr^i_2)_2]$.

The oxidation state formalism is a useful technique for categorizing transition metal complexes in terms of their oxidation levels and resultant d^n electronic configurations. While there are a number of ligands for which assignment of a formal charge can generate ambiguous results, for example, the nitrosyl and cycloheptatrienyl cations, this formalism has found widespread acceptance.¹ One particular use has been to recognize that there are gaps in our knowledge of particular metals in specific oxidation levels. For example, in the chemistry of the elements of group 4, one finds that for titanium, complexes of Ti^{III} and Ti^{IV} predominate which is in stark con-

trast to the heavier members of this group, namely zirconium and hafnium, for which the +4 oxidation state is dominant.^{2,3} In fact, coordination compounds of zirconium(III) and hafnium(III) are very poorly documented in the literature.⁴

One of the possible reasons for the rarity of the Zr^{III} state is due to the relatively large negative reduction potential for the Zr^{IV}/Zr^{III} couple. Reduction potentials for a variety of zirconocene derivatives range from $E^0 = -1.6$ V to $E^0 = -2.1$ V;⁵⁻⁸ by comparison, the analogous couple for similar complexes of titanium range from -0.75 to -1.5 V making the reduction of Zr^{IV} to Zr^{III} more difficult than the same reduction to Ti^{III} by approximately 1 V. While this does not generally present any technical difficulty, it does however suggest that

* Author to whom correspondence should be addressed.

certain precautions must be taken to ensure that this lower oxidation state of Zr, once formed, is kinetically stabilized. In addition, the tendency for metal-metal bond formation is more pronounced for the heavier members of a given triad in the transition series.² For example, careful reduction of zirconocene dihalides generally leads to the formation of diamagnetic dimers⁹⁻¹³ of the type $[\text{Cp}_2\text{Zr}]_2(\mu\text{-X})_2$ or fulvalene systems;¹⁴⁻¹⁷ in fact, many attempts to produce Zr^{III} species have resulted in the formation of dinuclear species that are diamagnetic.¹⁸⁻²²

Our interest in other oxidation states of the heavier group 4 elements, particularly zirconium, arose out of studies directed at the synthesis of dinitrogen complexes.^{23,24} Case in point, during the reduction of the mononuclear Zr^{IV} precursor $\text{Zr}(\eta^5\text{-C}_5\text{H}_5)\text{Cl}_2[\text{N}(\text{SiMe}_2\text{CH}_2\text{PPr}^i_2)_2]$ with Na/Hg to ultimately give the deep-brown-coloured dinuclear dinitrogen complex $\{[(\text{Pr}^i_2\text{PCH}_2\text{SiMe}_2)_2\text{N}]\text{Zr}(\eta^5\text{-C}_5\text{H}_5)\}_2(\mu\text{-N}_2)$, we noticed that a deep emerald green colouration persisted in solution for many hours before the final colour of the dinitrogen complex appeared. By reducing the time of the reduction, we were able to isolate in excellent yield a mononuclear Zr^{III} complex of the formula $\text{Zr}(\eta^5\text{-C}_5\text{H}_5)\text{Cl}[\text{N}(\text{SiMe}_2\text{CH}_2\text{PPr}^i_2)_2]$.²⁵ In this article we provide full details of the preparation, structure and reactivity of this Zr^{III} derivative. What emerges from this study is that the combination of a cyclopentadienyl unit and two bulky phosphine donors anchored by an amido ligand serves to stabilize mononuclear, paramagnetic complexes of Zr^{III} .

Background

In standard textbooks one can find references to trivalent halides of the formula ZrX_3 , where $\text{X} = \text{Cl}, \text{Br}$ and I , but these species are confined to solid-state studies.^{2,3} Adducts of these materials have been reported, but in general their characterization has been minimal or at least conflicting. For example, reactions of ZrX_3 with nitrogen donor ligands have been reported but the unusual stoichiometries and unexpected magnetic properties suggest dinuclear or oligonuclear structures. Poor

solubility has prevented resolution of the problem.²⁶⁻²⁹

Probably the first well-characterized formally Zr^{III} complexes were the dinuclear species prepared by reduction of ZrCl_4 in the presence of trialkylphosphines by Na/Hg.^{18,19} Dimeric complexes of the formula $[(\text{R}_3\text{P})_2\text{Cl}_2\text{Zr}]_2(\mu\text{-Cl})_2$ have been prepared and structurally characterized.^{20,21,30} Although these derivatives are diamagnetic, there is some evidence to suggest that in the presence of excess PR_3 , formation of a mononuclear, paramagnetic species is possible as evidenced by the observation of ESR signals. Other dinuclear complexes of the formula $[\text{Cp}_2\text{Zr}]_2(\mu\text{-X})_2$ are also known as well as fulvalene-bridged dinuclear species.^{9-16,22,31-35}

Interestingly enough, there is a vast literature concerning mononuclear, paramagnetic Zr^{III} complexes, but much of this work reports species that are generated in solution, for example, *in situ* in an ESR cavity or an electrochemical cell;^{5-8,35-49} until recently, there were few examples of isolable, mononuclear Zr^{III} complexes and, consequently, X-ray structural studies were lacking.^{13,50-54} The situation for hafnium is more pronounced as the Hf^{III} state is even rarer than that of Zr^{III} .^{4,21,38,50,55,56}

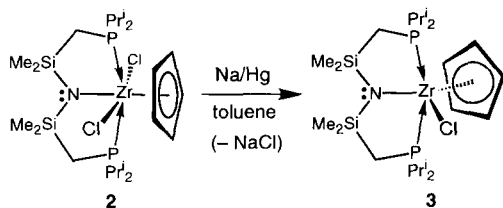
RESULTS AND DISCUSSION

Synthesis of zirconium(III) complexes

We have previously published the preparation of the dinuclear dinitrogen complex $\{[(\text{Pr}^i_2\text{PCH}_2\text{SiMe}_2)_2\text{N}]\text{Zr}(\eta^5\text{-C}_5\text{H}_5)\}_2(\mu\text{-N}_2)$ (**1**), by reduction of the Zr^{IV} precursor $\text{Zr}(\eta^5\text{-C}_5\text{H}_5)\text{Cl}_2[\text{N}(\text{SiMe}_2\text{CH}_2\text{PPr}^i_2)_2]$ (**2**) with excess sodium/amalgam (Na/Hg) under an atmosphere of dinitrogen.²⁴ During the course of this reaction the colour changes are rather noticeable as the pale yellow solution of **2** darkens upon reduction to a deep emerald green and finally to the dark brown colour characteristic of the dinitrogen complex **1**. When the same reduction was performed in the absence of N_2 , the deep green colour persisted indefinitely. By reducing the time of the reaction, excellent yields of a deep green crystalline material could be obtained [eq. (1)]. Elemental analyses were consistent with the empirical formula $\text{Zr}(\eta^5\text{-C}_5\text{H}_5)\text{Cl}[\text{N}(\text{SiMe}_2\text{CH}_2\text{PPr}^i_2)_2]$ (**3**); the complex did not display useful ^1H or $^{31}\text{P}\{^1\text{H}\}$ NMR spectra and the magnetic moment (μ_{eff} , Evan's method) was 1.57 B.M.* In addition, solutions displayed a strong isotropic ESR spectrum at ambient temperature consisting of a sharp binomial triplet at $g = 1.955$ with coupling to two phosphorus-31 nuclei and satellites due to one magnetically dilute zirconium

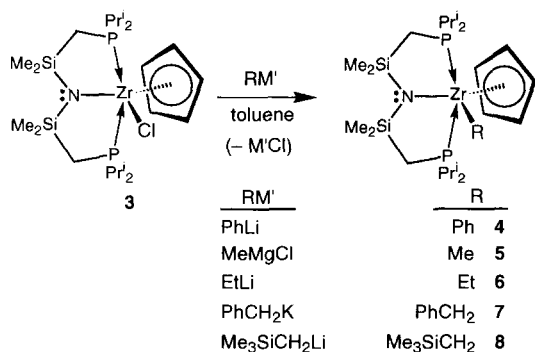
* This value is lower than the spin only value of 1.73 B. M. The lower magnetic moment could be attributed to magnetic exchange, i.e. some degree of association between mononuclear species; or to spin-orbit coupling. The calculated spin-orbit coupling constant of Zr^{3+} , 500 cm^{-1} , should give a magnetic moment of *ca* 1.2 B.M.⁵⁷ See B. N. Figgis and J. Lewis, *Prog. Inorg. Chem.* 1964, **6**, 37.

nucleus [$a(^{91}\text{Zr}) = 37.2$ G, ^{91}Zr , 11.23%, $I = 5/2$], all of which is consistent with a mononuclear species in solution. The ESR spectrum of **3** could be simulated using the following parameters: $a(^{31}\text{P}) = 21.1$ G, 2P; $a(^{14}\text{N}) = 2.9$ G, 1N; $a(^1\text{H}) = 1.8$ G, 5H; linewidth = 2.3 G.



The chloride complex **3** is indefinitely stable at room temperature in solution and in the solid-state in the absence of oxygen or moisture.

The remaining chloride of **3** can be metathesized by a variety of organometallic reagents as shown in eq. (2). Thus, reaction of PhLi with **3** at -78°C in toluene gives an instantaneous colour change from dark green to form a deep red solution from which diamond-shaped crystals could be obtained of the phenyl complex $\text{Zr}(\eta^5\text{-C}_5\text{H}_5)\text{Ph}[\text{N}(\text{SiMe}_2\text{CH}_2\text{PPr}_2)_2]$ (**4**). The solution (in toluene) ESR spectrum of complex **4** recorded at room temperature shows a broad binomial triplet at $g = 1.981$ due to coupling to two phosphorus-31 nuclei [$a(^{31}\text{P}) = 20.3$ G]; in addition, satellites due to the coupling of the dilute zirconium-91 nucleus were observed [$a(^{91}\text{Zr}) = 20.7$ G].



The zirconium(III) alkyl complexes $\text{Zr}(\eta^5\text{-C}_5\text{H}_5)\text{R}[\text{N}(\text{SiMe}_2\text{CH}_2\text{PPr}_2)_2]$, where R = Me (**5**), Et (**6**), PhCH₂ (**7**) and Me₃SiCH₂, (**8**), were synthesized using different alkyl transfer reagents [eq. (2)]. Unlike the dark red phenyl derivative, all of the alkyl derivatives are deep green in colour. Elemental analyses are given in the experimental section; however, isolation of micro-analytically pure samples of the complexes with small alkyl groups, that is, R = methyl (**5**) and R = ethyl (**6**),

was hampered by the apparent incorporation of MgCl₂ or LiCl in the samples. Table 1 gives the elemental compositions calculated and found for these hydrocarbyl derivatives along with the effect of various amounts of calculated metal halide salts. The presence of chloride is clearly indicated by the chloride analyses. The amount of added MgCl₂, 0.22 equiv, for the methyl **5** is arbitrary and was calculated on the basis of the low carbon and hydrogen elemental analyses found; no attempt was made to further substantiate this. For the ethyl **6** the analytical data for the crystals from the first recrystallization and from the second recrystallization appear to fit 0.6 and 0.2 equiv. of LiCl, respectively. Attempts to obtain MgCl₂ and LiCl free materials was not achieved even after repeated recrystallization attempts and addition of coordinating solvents such as dioxane.

It is known that certain zirconium(IV) complexes form adducts with LiCl,⁵⁸ a phenomenon that could be attributed to the Lewis acidity and to the coordinative unsaturation of the zirconium(IV) centre. Similar factors may be responsible for the incorporation of MgCl₂ and LiCl into the zirconium(III) complexes **5** and **6**, respectively. However, in these zirconium(III) derivatives, the interactions between the zirconium and the halide ion of the salts (i.e. LiCl or MgCl₂) are probably weak and become less favourable as the steric bulk of the alkyl group is increased; thus, for the phenyl complex **4** as well as the benzyl **7** and the trimethylsilylmethyl **8**, calculated and found elemental analyses were within acceptable limits for the metal-halide free materials. The room-temperature solution ESR spectra of sample of the ethyl complex **6**, formulated as **6**·(LiCl)_{0.6} and **6**·(LiCl)_{0.2}, were virtually identical and showed no hyperfine coupling to ⁶Li. It is noteworthy that the ESR spectrum of the anionic zirconium species $[\text{Cp}_2\text{Zr}(\text{CH}_2\text{SiMe}_3)_2]^- [\text{Na}(\text{THF})_3]^+$ did not show hyperfine interaction due to sodium;⁶ in contrast, the phosphide derivative $[\text{Cp}_2\text{Zr}(\text{PET}_2)_2]^- [\text{Na}(\text{THF})_3]^+$ does show hyperfine features due to the coupling of one ²³Na nucleus.³⁸

Solution magnetic studies (Evans Method) on the CH₂SiMe₃ derivative **8** gave a value of $\mu_{\text{eff}} = 1.73$ B.M., which is close to the calculated spin only value of a *d*¹ zirconium(III) centre. The room-temperature solution ESR spectra of the alkyl derivatives are more complicated than the spectrum of the phenyl derivative **4**. With the exception of the benzyl derivative, the hyperfine interaction of the unpaired electron with the two phosphorus nuclei are in the range of 20–21 G. In the case of the ethyl **6** and benzyl **7** derivatives, the satellites due to the zirconium-91 nucleus were not observed.

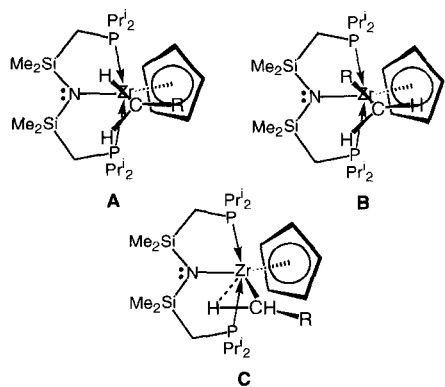
Table 1. Micro-analytical data for the methyl and ethyl derivatives $Zr(\eta^5-C_5H_5)Me[N(SiMe_2CH_2PPr^i_2)_2]$ (**5**) and $Zr(\eta^5-C_5H_5)Et[N(SiMe_2CH_2PPr^i_2)_2]$ (**6**)

Complex		C	H	N	Cl
$Zr(\eta^5-C_5H_5)Me[N(SiMe_2CH_2PPr^i_2)_2]$ (5)	Anal. Calc. for $C_{24}H_{52}NP_2Si_2Zr$	51.1	9.3	2.5	0.0
	Found	48.9	9.1	2.4	2.5
	Anal. Calc. for $C_{24}H_{52}NP_2Si_2Zr(MgCl_2)_{0.22}$	49.3	9.0	2.4	2.7
$Zr(\eta^5-C_5H_5)Et[N(SiMe_2CH_2PPr^i_2)_2]$ (6)	Anal. Calc. for $C_{25}H_{54}NP_2Si_2Zr$	51.9	9.4	2.4	0.0
	Found for first recrystallization	49.8	9.1	2.3	nd ^a
	Anal. Calc. for $C_{24}H_{52}NP_2Si_2Zr \cdot (LiCl)_{0.6}$	49.8	9.0	2.3	3.5
	Found for second recrystallization	51.2	9.3	2.4	nd ^a
	Anal. Calc. for $C_{24}H_{52}NP_2Si_2Zr \cdot (LiCl)_{0.2}$	51.2	9.3	2.4	1.21

^a nd = not done.

Simulation studies of the room-temperature solution (toluene) ESR spectrum of the methyl derivative **5** suggest that the three α -hydrogens of the methyl group attached to zirconium are isotropic. An intriguing feature in the ESR spectra of the ethyl and CH_2SiMe_3 derivatives is that the α -hydrogens have different hyperfine coupling constants. This difference in hyperfine interaction could be due to restricted rotation about the zirconium-carbon bond associated with the alkyl substitution.^{59,60} If the rotation is slow on the ESR time scale, some rotational isomers would have a longer lifetimes than the others. Scheme 1 shows the two types of conformational isomers for the ethyl and the CH_2SiMe_3 derivatives, where type **A** has enantiotopic α -hydrogens, and type **B** has diastereotopic α -hydrogens. The diastereotopic α -hydrogens of conformer **B** could in principle have different hyperfine coupling constants.

An alternative explanation for the different coup-



Scheme 1.

ling constants for the α -hydrogens would be that, in solution, one of the α -hydrogens weakly interacts with the paramagnetic metal centre to generate an α -agostic type structure shown as **C**.^{61,62} Although no evidence for this was found in the solid-state structure (*vide infra*), such an interaction is well known for early transition metal complexes.⁶¹ Attempts to detect this proposed interaction by IR studies were not conclusive since there is extensive overlap in the C—H stretching region due to the ancillary ligand.

The solution ESR spectrum of the benzyl zirconium(III) derivative **7** does not have a centre of symmetry, which suggests that more than one species exist in solution. It is possible that the benzyl ligand is coordinated in an η^2 -fashion,⁶³ or with a geometry similar to **C** above. The latter geometry would make the two benzylic protons diastereotopic, and this proposal is consistent with the hyperfine values obtained (by simulation) for the α -hydrogens.

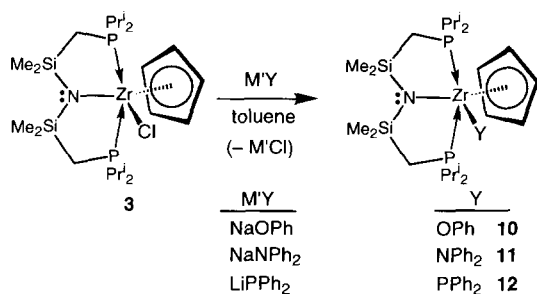
The formation of the benzyl complex from the starting chloro complex **3** was found to be capricious depending on the benzylating agent. For example, the use of the Grignard, $(PhCH_2)MgCl$, led to the formation of a diamagnetic side product shown to be $ZrCl(CH_2Ph)_2[N(SiMe_2CH_2PPr^i_2)_2]$ (**9**), in approximately 20% isolated yield, presumably by displacement of C_5H_5 followed by disproportionation of the resulting Zr^{III} complex $Zr(CH_2Ph)Cl[N(SiMe_2CH_2PPr^i_2)_2]$. Although **9** was never formed as the major product, it did tend to complicate isolation of the Zr^{III} benzyl derivative. The use of potassium benzyl, KCH_2Ph , allowed straightforward isolation of the paramagnetic benzyl complex without observation of diamagnetic side products.

Table 2. Hyperfine coupling constants^a (G) for the chloro and the hydrocarbyl derivatives of $Zr(\eta^5-C_5H_5)R[N(SiMe_2CH_2PPr^i_2)_2]$

R	<i>g</i>	<i>a</i> (⁹¹ Zr)	<i>a</i> (³¹ P)	<i>a</i> (¹⁴ N)	<i>a</i> (¹ H _z)	<i>a</i> (¹ H _β)	<i>a</i> (¹ H _{CP})
Cl (3)	1.955	37.2	21.1	2.9			1.8
C ₆ H ₅ (4)	1.981	20.7	20.3	1.8			1.1
CH ₃ (5)	1.963	28.0	21.1	2.1	6.6		
CH ₂ CH ₃ (6)	1.962		20.9	2.6	9.3	3.2	1.8
CH ₂ C ₆ H ₅ ^b (7)	1.956		18.6	3.4	3.2		1.2
CH ₂ Si(CH ₃) ₃ (8)	1.973	30.5	21.4	2.0	9.3	6.2	

^a All the values were obtained from simulations as described in the Experimental section. Although some of the line-widths used in the simulations were on the order of the hyperfine coupling constant *a*(¹⁴N), other combinations did not result in any better agreement.

^b The hyperfine values given for the benzyl derivative are only approximate values.



Synthesis of hafnium(III) complexes

The reduction of the hafnium(IV) precursor $Hf(\eta^5-C_5H_5)Cl_2[N(SiMe_2CH_2PPr^i_2)_2]$ (**13**) with Na/Hg gave a brown material, from which deep brown crystalline cubes were isolated by recrystallization. The ESR spectrum of the initially recrystallized material consisted of a triplet and a broad singlet; the triplet resonance was identical to the resonance of the zirconium(III) complex **3** (Fig. 1) as shown conclusively by overlapping the spectrum with an authentic sample of **3**. The broad signal³⁸ is assigned to the hafnium(III) species $Hf(\eta^5-C_5H_5)Cl[N(SiMe_2CH_2PPr^i_2)_2]$ (**14**). As will be shown later, this sample consists mainly of the hafnium(III) complex **14** in approximately 10:1 ratio with the Zr^{III} impurity of **3**.

Commercially available hafnium precursors (e.g. $HfCl_4$) contain zirconium impurities in the range 1–4%. Therefore, most organometallic complexes of hafnium are likely to have a very small percentage of the zirconium analogue as an impurity, as has been noted previously.^{50,55,56} During the reduction of the hafnium(IV) derivatives the hafnium intermediates possibly undergo decomposition at a higher rate than the zirconium counterparts, which could eventually lead to the enrichment of the zirconium analogue in the product. The presence of zirconium impurities would also hamper the isolation of analytically pure hafnium(III) samples (Table 3). In our case, isolation of the analytically pure hafnium(III) complex **14** was possible, but this may have been fortuitous. The initial crystallization gave a material for which carbon and hydrogen analyses were off by 1–2%; a second crystallization did produce an analytically pure sample but this was accompanied by the formation of the dinuclear dinitrogen complex of zirconium, **1** [by ³¹P{¹H} NMR spectroscopy]. It could be that

Besides the hydrocarbyl species shown in eq. (2), the synthesis of Zr^{III} complexes with a heteroatom directly bonded to zirconium could be achieved; thus metathesis of the zirconium(III) chloride complex **3** with 1 equiv. of NaOPh, NaNPh₂ or LiPPh₂ led to the synthesis of $Zr(\eta^5-C_5H_5)OPh[N(SiMe_2CH_2PPr^i_2)_2]$ (**10**), $Zr(\eta^5-C_5H_5)NPh_2[N(SiMe_2CH_2PPr^i_2)_2]$ (**11**) and $Zr(\eta^5-C_5H_5)PPh_2[N(SiMe_2CH_2PPr^i_2)_2]$ (**12**), respectively [eq. (3)]. The phenoxy derivative was deep green in colour, whereas the amido and the phosphido derivatives gave dark brown solutions. These complexes were extremely soluble in hydrocarbon solvents and only the phenoxy derivative was isolated in a solid form amenable to elemental analysis. However, the ESR spectra of the crude samples were symmetric, and the ¹H NMR spectra showed only broad peaks, suggesting that the synthesis of these complexes proceeds in virtually quantitative yields. The room-temperature solution ESR spectra of the amido derivative, **11** [*g* = 1.953, *a*(³¹P) = 11.2 G], and the phenoxy derivative, **10** [*g* = 1.955, *a*(³¹P) = 18.7 G], consist of a broad binomial triplet indicating coupling of 2 equiv. phosphorus nuclei. The phosphido derivative **12** displays a doublet of triplets [*g* = 1.965; *a*(³¹P) = 29.8 G, 1P; *a*(³¹P) = 18.6 G, 2P], which is consistent with a mononuclear zirconium species.³⁸

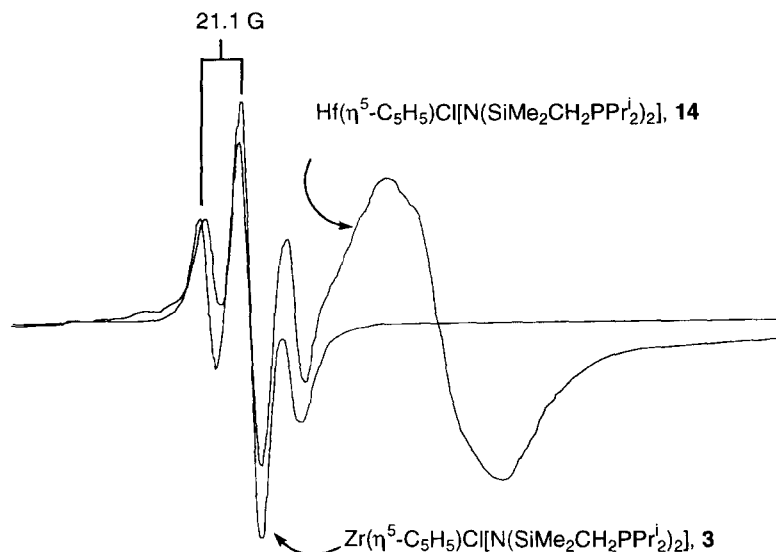


Fig. 1. Overlapping room-temperature ESR spectra of a solution (toluene) sample of $\text{Hf}(\eta^5\text{-C}_5\text{H}_5)\text{Cl}[\text{N}(\text{SiMe}_2\text{CH}_2\text{PPr}^i_2)_2]$ (**14**) and $\text{Zr}(\eta^5\text{-C}_5\text{H}_5)\text{Cl}[\text{N}(\text{SiMe}_2\text{CH}_2\text{PPr}^i_2)_2]$ (**3**).

Table 3. Elemental composition found for some hafnium(III) derivatives

Complex		C	H	Other	References
$\text{Hf}(\eta^5\text{-C}_5\text{H}_5)\text{Cl}[\text{N}(\text{SiMe}_2\text{CH}_2\text{PPr}^i_2)_2]$ (14)	Calc.	41.1	7.3	N	This work
	Found	41.5	7.5	2.1	
$[\text{HfCl}_3(\text{dippe})_2]$				Cl	56
	Calc.	30.7	5.9	19.4	
$\text{Hf}(\eta^5\text{-C}_5\text{Me}_5)(\eta^7\text{-C}_7\text{H}_7)$				Hf	50
	Found	31.7	6.0	18.3	
$\text{Hf}(\eta^5\text{-C}_5\text{Me}_5)(\eta^7\text{-C}_7\text{H}_7)$	Calc.	50.4	5.5	44.1	50
	Found	51.9	5.6	44.5	

the Hf^{III} complex can further reduce the corresponding Zr^{III} impurity **3** upon standing under N_2 to the less soluble dinuclear dinitrogen complex, thereby removing the Zr impurity. To our knowledge this is the first hafnium(III) complex that has been characterized by satisfactory microanalyses. Further reactions of the Hf^{III} chloride complex $\text{Hf}(\eta^5\text{-C}_5\text{H}_5)\text{Cl}[\text{N}(\text{SiMe}_2\text{CH}_2\text{PPr}^i_2)_2]$ (**14**) have not yet been carried out.

Structural studies

Both the phenyl complex, $\text{Zr}(\eta^5\text{-C}_5\text{H}_5)\text{Ph}[\text{N}(\text{SiMe}_2\text{CH}_2\text{PPr}^i_2)_2]$ (**4**), and the trimethylsilylmethyl derivative, $\text{Zr}(\eta^5\text{-C}_5\text{H}_5)\text{CH}_2\text{SiMe}_3[\text{N}(\text{SiMe}_2\text{CH}_2\text{PPr}^i_2)_2]$ (**8**), were obtained in single crystalline form to allow analysis by X-ray diffraction. The molecular structures and numbering schemes of **4** and **8**

are shown in Fig. 2. These two examples are the first structurally characterized, mononuclear derivatives of zirconium(III) containing a σ -hydrocarbyl ligand.²⁵

The structural parameters (Tables 4 and 5) associated with the PNP ligand in both derivatives are similar to zirconium(IV) complexes previously published by us.^{24,64-67} A comparison of bond angles around the zirconium centres suggests that the coordination environment can be envisaged as a distorted trigonal bipyramid with the phosphine donors of the meridionally coordinated PNP ligand occupying the axial positions. The equatorial ligands are therefore the centroid of the cyclopentadienyl unit, the amide donor of the tridentate ligand and the hydrocarbyl group. The structure shows that the backbone of the tridentate ligand is twisted. The distances from the zirconium to the

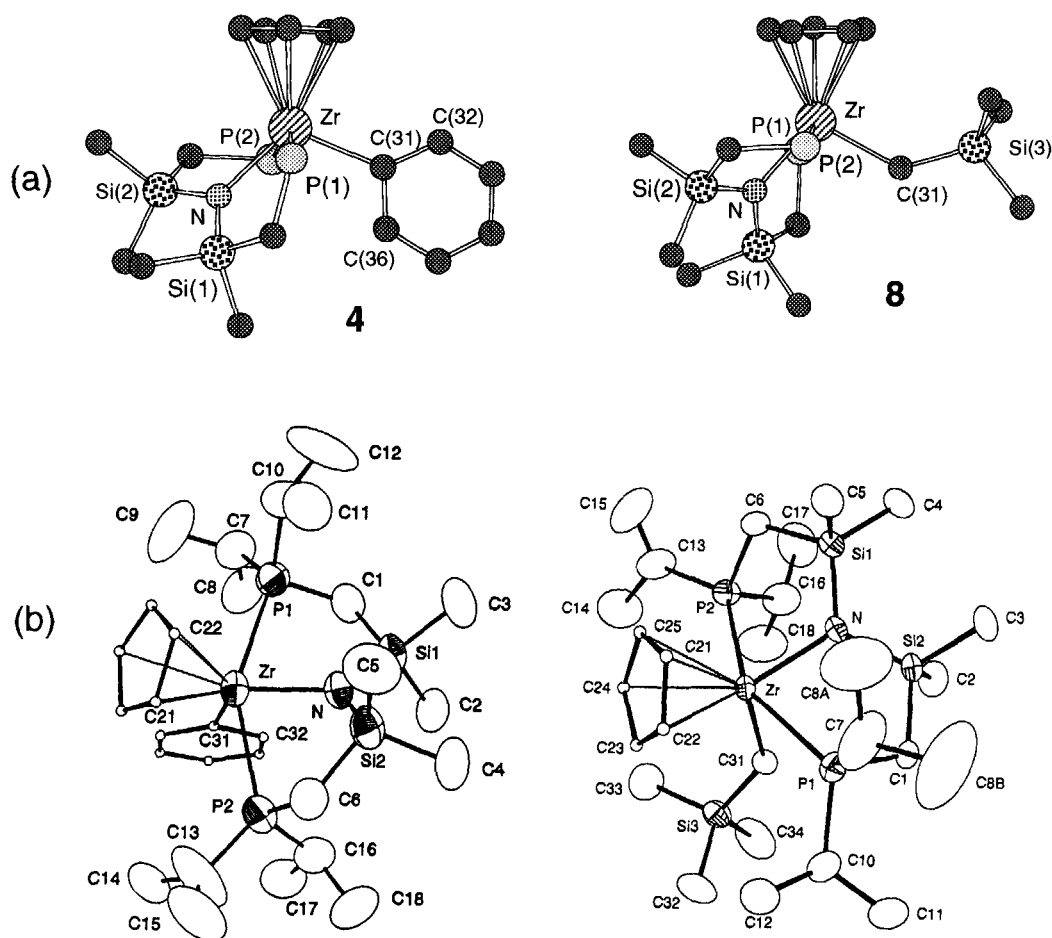


Fig. 2. (a) Chem 3D views of $Zr(\eta^5-C_5H_5)Ph[N(SiMe_2CH_2PPr_2)_2]$ (**4**) (top), and $Zr(\eta^5-C_5H_5)CH_2SiMe_3[N(SiMe_2CH_2PPr_2)_2]$ (**8**) (bottom); only selected atoms have been labelled. The isopropyl substituents on the phosphorus donors have been omitted for clarity; (b) ORTEP views with all atoms shown and labelled.

centroid of the Cp ligand in the phenyl, **4** (2.225 Å), and the alkyl, **8** (2.2162 (5) Å), derivatives are slightly shorter (the difference is greater than 0.05 Å) than the distances observed for the dinuclear dinitrogen zirconium(IV) derivative **1** (2.286 and 2.294 Å).

The zirconium–carbon bond distances associated with the phenyl, **4** [2.272 (3) Å], and the alkyl, **8** [2.337 (5) Å], derivatives are within the observed range for zirconium complexes containing bulky alkyl groups, for example in $(\eta^5-C_5H_5)_2ZrPh[CH(SiMe_3)_2]$ the zirconium– C_{ipso} and zirconium– $C(\text{alkyl})$ distances are 2.324 (7) and 2.329 (6) Å, respectively. For zirconocene derivatives the zirconium– $C(sp^3)$ bond distances range from 2.251 (6) to 2.388 (12) Å, where the longer distances are associated with larger alkyl groups. In the PNP derivative $Zr(\eta^4-C_4H_6)Ph[N(SiMe_2CH_2PPr_2)_2]$, the zirconium– C_{ipso} distance of 2.317 (7) Å is slightly

longer than that observed in the zirconium(III) phenyl derivative, **4**.

The bond angles between the zirconium, *ipso*-carbon and the *ortho*-carbons in $Zr(\eta^4-C_4H_6)Ph[N(SiMe_2CH_2PPr_2)_2]$ are similar being 121.1 (6) and 125.3(6)°,⁶⁷ however, the comparable angles in the zirconium(III) phenyl complex **4**, $Zr-C(31)-C(36)$ and $Zr-C(31)-C(32)$, are 132.5 (5) and 114.9(3)°, which is a remarkably large difference; this is shown in Fig. 3. These angle parameters seem to suggest that in **4** the phenyl ligand is skewed about the *ipso*-carbon towards the amide donor of the tridentate ancillary ligand. The phenyl group in complex **4** is coplanar with the equatorial plane of the distorted trigonal bipyramidal geometry of the complex described above and therefore might be expected to experience some steric interactions with the Cp ligand, where the centroid of the Cp ligand also lies in this same equatorial

Table 4 Selected bond lengths (Å) of complexes $\text{Zr}(\eta^5\text{-C}_5\text{H}_5)\text{Ph}[\text{N}(\text{SiMe}_2\text{CH}_2\text{PPr}^i_2)_2]$ (**4**) and $\text{Zr}(\eta^5\text{-C}_5\text{H}_5)\text{CH}_2\text{SiMe}_3[\text{N}(\text{SiMe}_2\text{CH}_2\text{PPr}^i_2)_2]$ (**8**)

$\text{Zr}(\eta^5\text{-C}_5\text{H}_5)\text{Ph}[\text{N}(\text{SiMe}_2\text{CH}_2\text{PPr}^i_2)_2]$ (4)		$\text{Zr}(\eta^5\text{-C}_5\text{H}_5)\text{CH}_2\text{SiMe}_3[\text{N}(\text{SiMe}_2\text{CH}_2\text{PPr}^i_2)_2]$ (8)	
Zr—P(1)	2.7819(14)	Zr—P(1)	2.7923(16)
Zr—P(2)	2.7843(16)	Zr—P(2)	2.8563(17)
Zr—N	2.231(3)	Zr—N	2.216(4)
Zr—C(31)	2.272(4)	Zr—C(31)	2.337(5)
Zr—Cp	2.225	Zr—Cp	2.2162(5)

Table 5. Selected bond angles^a (°) for the complexes $\text{Zr}(\eta^5\text{-C}_5\text{H}_5)\text{Ph}[\text{N}(\text{SiMe}_2\text{CH}_2\text{PPr}^i_2)_2]$ (**4**) and $\text{Zr}(\eta^5\text{-C}_5\text{H}_5)\text{CH}_2\text{SiMe}_3[\text{N}(\text{SiMe}_2\text{CH}_2\text{PPr}^i_2)_2]$ (**8**)

$\text{Zr}(\eta^5\text{-C}_5\text{H}_5)\text{Ph}[\text{N}(\text{SiMe}_2\text{CH}_2\text{PPr}^i_2)_2]$ (4)		$\text{Zr}(\eta^5\text{-C}_5\text{H}_5)\text{CH}_2\text{SiMe}_3[\text{N}(\text{SiMe}_2\text{CH}_2\text{PPr}^i_2)_2]$ (8)	
P(1)—Zr—P(2)	150.09(4)	P(1)—Zr—P(2)	151.17(5)
P(1)—Zr—N	79.47(9)	P(1)—Zr—N	77.83(11)
P(2)—Zr—N	75.01(10)	P(2)—Zr—N	74.37(11)
P(1)—Zr—C(31)	87.04(11)	P(1)—Zr—C(31)	85.13(13)
P(2)—Zr—C(31)	88.57(11)	P(2)—Zr—C(31)	93.47(13)
P(1)—Zr—Cp	104.27	P(1)—Zr—Cp	103.95(4)
P(2)—Zr—Cp	104.82	P(2)—Zr—Cp	102.08(4)
N—Zr—C(31)	112.60(13)	N—Zr—C(31)	102.47(16)
N—Zr—Cp	135.57	N—Zr—Cp	139.47(10)
C(31)—Zr—Cp	111.81	C(31)—Zr—Cp	118.05(13)
Zr—C(31)—C(36)	132.5(5)	Zr—C(31)—Si(3)	134.0(3)
Zr—C(31)—C(32)	114.9(3)	Si(1)—N—Si(2)	120.18(23)
Si(1)—N—Si(2)	119.15(17)		

^aCp refers to the centroid of the Cp ligand. All structural parameters associated with the Cp ligand for the complex **4** were taken from the Chem 3D[®] structure.

plane. Yet another explanation might be that the *ortho*-C—H on C(36) is interacting to some extent with the coordinatively unsaturated Zr^{III} centre in a β -agostic type interaction.

As previously mentioned, we calculated different

α -C—H hyperfine coupling constants for the ethyl **6** and trimethylsilylmethyl derivatives **8**; one possible rationale for this would be the presence of an α -agostic interaction. Although the C—H's on the trimethylsilylmethyl ligand could not be located in

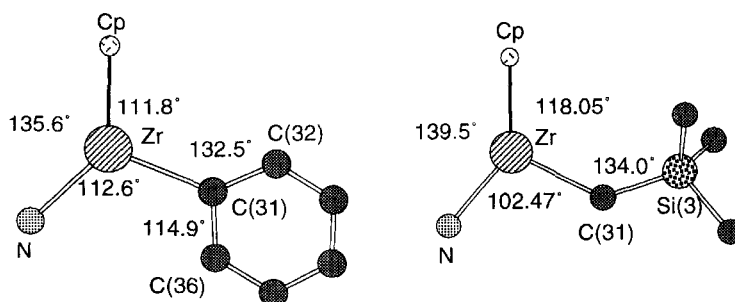
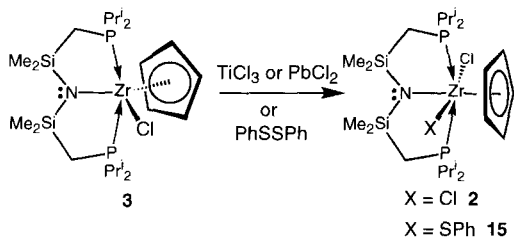


Fig. 3. The core models of the phenyl **4** and trimethylsilylmethyl **8** complexes that show the angles in the trigonal plane of the structures; most of the substituents have been omitted for clarity (the atom labelled Cp refers to the centroid).

the solid-state structure of **8**, the large Zr—C(31)—Si(3) bond angle of 134.0(3)° might be indicative of such an interaction (Fig. 3). However, this angle could be due, again, to the steric constraints of the coordination sphere due to the interaction of the Cp ligand with the silylmethyl groups. The recent report of the Zr^{III} porphyrin derivative Zr(CH₂SiMe₃)[OEP] shows a smaller Zr—C—Si angle of 124.1(4)° probably due to the less sterically crowded nature of the coordination environment.⁵⁴

Oxidation of zirconium(III) complexes

Treating a solution of zirconium(III) chloro derivative **3** with solid TiCl₃ or PbCl₂ led to the oxidation⁶⁸ of the zirconium complex to give the starting dichloro zirconium(IV) complex **2** in almost quantitative yield. Also, 0.5 equiv. of PhS-SPh react with complex **3** to give the zirconium(IV) thiolate derivative, Zr(η⁵-C₅H₅)(SPh)Cl[N(SiMe₂CH₂PPr₂)₂] (**15**), in quantitative yields [eq. (4)]. These reactions have been useful in quantifying the purity of some zirconium(III) derivatives. For example, during the synthesis of the alkyl complex Zr(η⁵-C₅H₅)CH₂SiMe₃[N(SiMe₂CH₂PPr₂)₂] (**8**) an aliquot of the crude reaction mixture was titrated against a solution of PhSSPh, where a colour change occurs from deep green to yellow. The resulting solution could then be analysed by ³¹P{¹H} NMR spectroscopy to show that the metathesis reactions involving **3** and various alkyl transfer reagents proceed in almost quantitative (>95%) yields.



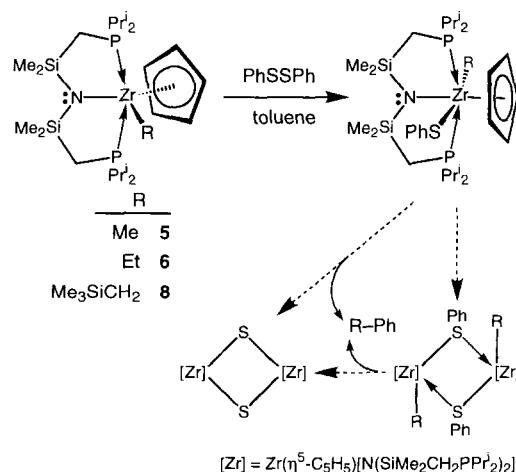
Oxidation of a crude sample of the hafnium(III) chloro derivative **14** with TiCl₃ followed by NMR analysis showed the presence of the dichlorides of hafnium(IV) and zirconium(IV) in an approximately 10:1 ratio. This result is consistent with the previous suggestion that during the reduction of the hafnium(IV) precursor the ratio of the zirconium impurity increases as shown in Fig. 1.

It is noteworthy that the oxidized monoalkyl derivatives, i.e. alkylthiolate and the alkylchloro complexes, Zr(η⁵-C₅H₅)XR[N(SiMe₂CH₂PPr₂)₂], where X = SPh and R = Me, Et or CH₂SiMe₃ or X = Cl and R = Me, Et or Bz, show broad res-

onances in their NMR spectra, suggesting these molecules are fluxional. The alkylchloro derivatives could be isolated as solid materials and were found to be thermally labile. The alkylthiolate derivatives are oils at room temperature and undergo further reaction to give a material which has complex ¹H NMR spectra. Also, the ³¹P{¹H} NMR spectra of these materials were virtually identical for all three derivatives, consisting of two low-field and two high-field singlets around 19 and -2 ppm, respectively. The NMR spectral features are possibly a result of an unsymmetrical dimeric species, containing bridging sulphido ligands⁶⁹ possibly a result of dimerization and alkane elimination (Scheme 2). However, more investigation is required to confirm the nature of this diamagnetic complex.

CONCLUSIONS

By suitably modifying the ancillary ligands around the zirconium and hafnium centres one can stabilize the rare trivalent state of these elements. Moreover, we have been able to isolate mononuclear, paramagnetic complexes with hydrocarbyl ligands directly bonded to Zr. In our particular case, the use of the tridentate amido-diphosphine ligand N(SiMe₂CH₂PPr₂)₂ is evidently an important component of the stabilization of this oxidation state since it provides the necessary steric protection to prevent aggregation and metal-metal bond formation. Given that phosphine donors are known to stabilize a variety of oxidation states of the later transition elements, an additional aspect to be considered is that the phosphine donors also provide the correct electronic environment for this lower oxidation state of Zr.



Scheme 2.

EXPERIMENTAL

General

The ^1H , ^{31}P and ^{13}C NMR spectra were recorded on a Varian XL-300, a Bruker AC-200, a Bruker WH-400 or a Bruker AM-500 spectrometer. Proton spectra were referenced using the partially deuterated solvent peak as the internal reference, $\text{C}_6\text{D}_5\text{H}$ at 7.15 ppm and $\text{C}_6\text{D}_5\text{CD}_2\text{H}$ at 2.09 ppm relative to Me_4Si . The $^{31}\text{P}\{^1\text{H}\}$ NMR spectra were referenced to external $\text{P}(\text{OMe})_3$ set at +141.00 ppm relative to 85% H_3PO_4 . The $^{13}\text{C}\{^1\text{H}\}$ NMR spectra were referenced to the C_6D_6 signal at 128.0 ppm or to the $\text{CD}_3\text{C}_6\text{D}_5$ signal at 20.4 ppm. $^1\text{H}\{^{31}\text{P}\}$ NMR spectra were recorded on the Bruker AM 500 spectrometer.

UV-vis spectra were recorded on a Perkin-Elmer 5523 UV-vis spectrophotometer stabilized at 20 °C. Mass spectral studies were carried out on a Kratos MS 50 using an EI source. IR spectra were recorded on a Bomem MB-100 spectrometer. Solution samples were recorded in a 0.1 mm KBr cell and solid samples were recorded as KBr pellets. Carbon, hydrogen, nitrogen and chloride analyses were performed by the microanalyst of this department.

Phenyllithium,⁷⁰ ethyllithium,⁷¹ benzylpotassium,⁷² $\text{LiCH}_2\text{SiMe}_3$,⁷³ $\text{NaCp} \cdot \text{DME}$ ⁷⁴ and dibenzylmagnesium⁷⁵ were prepared according to literature procedures. Methylmagnesium bromide (1.4 M solution in 75% toluene and 25% THF), benzylmagnesium chloride (1 M solution in Et_2O), CH_3CN , TiCl_3 , Ph_2S_2 and PbCl_2 were purchased from Aldrich. Diphenyldisulphide was purified by sublimation, acetonitrile was dried over 4 Å activated molecular sieves for 12 h and then vacuum transferred and degassed by three freeze-pump-thaw cycles. Lead(II) dichloride was pumped under vacuum for 24 h prior to use.

The ESR spectra were recorded on Varian E-3 spectrometer calibrated with a sample of $\text{VO}(\text{acac})_2$, $g = 1.965$. ESR simulations were done on a Macintosh Iix using ESR II from Calleo Scientific Software. The values of line broadening and coupling constants were obtained from the simulated spectra.

Both $\text{Zr}(\eta^5\text{-C}_5\text{H}_5)\text{Cl}_2[\text{N}(\text{SiMe}_2\text{CH}_2\text{PPr}^i_2)_2]$ (1) and $\text{HfCl}_3[\text{N}(\text{SiMe}_2\text{CH}_2\text{PPr}^i_2)_2]$ were prepared according to the published procedures.^{24,64}

Synthesis of complexes

$\text{Zr}(\eta^5\text{-C}_5\text{H}_5)\text{Cl}[\text{N}(\text{SiMe}_2\text{CH}_2\text{PPr}^i_2)_2]$ (3). A solution of $\text{Zr}(\eta^5\text{-C}_5\text{H}_5)\text{Cl}_2[\text{N}(\text{SiMe}_2\text{CH}_2\text{PPr}^i_2)_2]$ (2) (1.50 g, 2.42 mmol) in toluene (80 cm³) was transferred into a thick-walled reaction flask containing

Na/Hg (100 g of 0.3% amalgam, 13.0 mmol). The flask was then evacuated (3 min) and sealed. Upon stirring the reaction mixture turns deep green. After 48 h the reaction mixture was decanted from the amalgam and filtered through a layer of Celite[®]. The amalgam was extracted with 20 cm³ portions of hexanes (total of 60 cm³) until the washings showed no green colour. Upon removal of the solvent from the combined filtrate and extracts a dark green solid was obtained (95%). ESR spectrum of this green solid shows only the presence of 3 and ^1H NMR shows <5% (estimated relative to the amount of $\text{C}_6\text{D}_5\text{H}$ present in C_6D_6) diamagnetic impurities. Recrystallization from hexanes gave analytically pure material (1.25 g, 88%). ESR (toluene): $g = 1.955$; $a(^{91}\text{Zr}) = 37.2$ G, 1Zr; $a(^{31}\text{P}) = 21.1$ G, 2P; $a(^{14}\text{N}) = 2.9$ G, 1N; $a(^1\text{H}) = 1.8$ G, 5H; linewidth used for simulation, 2.3 G. μ_{eff} (Evans method) = 1.57 B. M. UV-vis (toluene, 1 cm quartz cell): $\lambda_{\text{max}} = 324$ nm, $\epsilon_{\text{max}} = 2600$ dm³ mol⁻¹ cm⁻¹; $\lambda = 360$ nm, $\epsilon = 2500$ dm³ mol⁻¹ cm⁻¹. Found: C, 47.0; H, 9.0; N, 2.2. Calc. for $\text{C}_{23}\text{H}_{49}\text{ClNP}_2\text{Si}_2\text{Zr}$: C, 47.3; H, 8.4; N, 2.49.

$\text{Zr}(\eta^5\text{-C}_5\text{H}_5)\text{C}_6\text{H}_5[\text{N}(\text{SiMe}_2\text{CH}_2\text{PPr}^i_2)_2]$, (4). To a solution of 3 (240 mg, 0.41 mmol) in toluene (5 cm³) was added PhLi (1.6 cm³ of 0.25 M solution in Et_2O , 0.40 mmol) at -78 °C and stirred for 5 min. After stirring the reaction at room temperature for 3 h the solvent was removed under vacuum. The deep brown residue was extracted with pentane (20 cm³) and the extract was filtered through Celite[®]. The filtrate was concentrated (2 cm³) and then cooled at -40 °C to give hexagonally shaped crystals (190 mg, 74%). ESR (toluene): $g = 1.981$; $a(^{91}\text{Zr}) = 20.7$ G, 1Zr; $a(^{31}\text{P}) = 20.3$ G, 2P; $a(^{14}\text{N}) = 1.8$ G, 1N; $a(^1\text{H}) = 1.1$ G, 5H; linewidth used for simulation, 2.8 G. UV-vis (toluene, 1 cm quartz cell): $\lambda_{\text{max}} = 342$ nm; $\lambda_{\text{max}} = 478$ nm. Found: C, 55.5; H, 8.7; N, 2.3. Calc. for $\text{C}_{29}\text{H}_{54}\text{N Si}_2\text{P}_2\text{Zr}$: C, 55.6; H, 8.7; N, 2.2%.

$\text{Zr}(\eta^5\text{-C}_5\text{H}_5)\text{Me}[\text{N}(\text{SiMe}_2\text{CH}_2\text{PPr}^i_2)_2]$ (5). To a solution of 3 (825 mg, 1.46 mmol) in toluene (25 cm³) was added a solution of MeMgX (X = Br, 1.1 cm³ of 1.4 M solution, 1.54 mmol; X = Cl, 0.55 cm³ of 3.0 M solution in THF, 1.6 mmol) at room temperature. The reaction mixture was stirred for 4 h and then the solvent was stripped off under reduced pressure. The resulting solid was extracted with pentane (10 cm³) and the extract was filtered through a layer of Celite[®]. The filtrate was concentrated (~3 cm³) and then cooled at -40 °C to give a deep green crystalline product (480 mg, 58%). ESR (toluene): $g = 1.963$; $a(^{91}\text{Zr}) = 28.0$ G, 1Zr; $a(^{31}\text{P}) = 21.1$ G, 2P; $a(^1\text{H}) = 6.6$ G, 3H; $a(^{14}\text{N}) = 2.1$ G, 1N; linewidth used for simulation,

3.0 G. Found: C, 48.9; H, 9.1; N, 2.4; Cl, 2.5. Calc. for $C_{24}H_{52}NP_2Si_2Zr(MgCl_2)_{0.22}$: C, 49.3; H, 9.0; N, 2.4; Cl 2.7%.

$Zr(\eta^5-C_5H_5)CH_2CH_3[N(SiMe_2CH_2PPr^i_2)_2]$ (6). Method 1: To a solution of **3** (1.00 g, 1.71 mmol) in toluene (25 cm³) was added a solution of CH_3CH_2Li (70 mg, 1.94 mmol) in toluene (10 cm³) at $-78^\circ C$. The reaction mixture was allowed to warm to room temperature and stirred for 8 h. The solvent was stripped off *in vacuo*, the residue was extracted with pentane (10 cm³) and the extract was filtered through a layer of Celite[®]. The filtrate was concentrated (3 cm³) and then cooled to $-40^\circ C$ to give a deep green crystalline product (560 mg, 56%). ESR (toluene): $g = 1.962$; $a(^{31}P) = 20.9$ G, 2P; $a(^1H_z) = 9.3$ G, 1H; $a(^1H_x) = 3.2$ G, 1H; $a(^1H_\beta) = 1.8$ G, 3H; $a(^{14}N) = 2.6$ G, 1N; linewidth used for simulation, 2.2 G. Found: (a) C, 49.8; H, 9.0; N, 2.3; (b) C, 51.2; H 9.3; N 2.4. Calc. for $C_{25}H_{54}NP_2Si_2Zr$: C, 51.9; H, 9.4; N, 2.4%. Case (a) was obtained from the first recrystallization and case (b) was obtained from the second recrystallization and the data seems to fit for 0.6 and 0.2 equiv. of LiCl, respectively.

$Zr(\eta^5-C_5H_5)CH_2Ph[N(SiMe_2CH_2PPr^i_2)_2]$ (7). To a solution of **3** (315 mg, 0.57 mmol) in THF (20 cm³) was added a solution of $PhCH_2K$ (70 mg, 0.54 mmol) in THF (5 cm³) at $-40^\circ C$. The reaction was warmed to room temperature and stirred for 5 h. The solvent was stripped off *in vacuo*, and the resulting solid was extracted with hexanes (10 cm³). The extract was filtered through a layer of Celite[®], concentrated (~ 3 cm³) and cooled at $-40^\circ C$ to give a dark green crystalline product (275 mg, 75%). ESR (toluene): $g = 1.956$; $a(^{31}P) = 18.6$ G, 2P; $a(^1H_z) = 3.2$ G, 2H; $a(^{14}N) = 3.4$ G, 1N; $a(^1H) = 1.2$ G, 5H linewidth used for simulation, 1.6 G. Found: C, 56.6; H, 8.9; N, 2.2. Calc. for $C_{30}H_{56}NP_2Si_2Zr$: C, 56.3; H, 8.8; N, 2.2%.

$ZrCl(CH_2Ph)_2[N(SiMe_2CH_2PPr^i_2)_2]$ (9). To a solution of **3** (350 mg, 0.6 mmol) in toluene (30 cm³) was added a solution of $PhCH_2MgCl$ (0.6 cm³ of 1 M solution in Et₂O, 0.6 mmol) at room temperature and stirred for 6 h. The solvent was stripped off *in vacuo*, the resulting solid was extracted with toluene (10 cm³) and filtered through a layer of Celite[®]. The filtrate was concentrated (1 cm³), and added hexanes (10 cm³) and cooling at $-40^\circ C$ gave a pale yellow material (63 mg, 15%). Upon further recrystallization the zirconium(III)-benzyl derivative **7** was isolated. ¹H NMR (δ , 300 MHz, C₆D₆): 0.18 [s, 6H, Si(CH₃)₂]; 0.45 [s, 6H, Si(CH₃)₂]; 0.6 (m, 4H, SiCH₂P); 0.8 to 1.0 (m, 24H, P[CH(CH₃)₂]₂); 1.60 (sept, 2H, P[CH(CH₃)₂]₂), ³J(H—H) = 6.3 Hz); 1.70 (sept, 2H, P[CH(CH₃)₂]₂), ³J(H—H) = 7.5 Hz); 1.98 (s,

2H, CH₂Ph); 2.02 (s, 2H, CH₂Ph); 6.87 [t, 2H, *p*-Ph, ³J(H—H) = 6.6 Hz]; 7.23 (m, 4H, *m*-Ph); 7.37 [d, 4H, *o*-Ph, ³J(H—H) = 6.6 Hz]. ³¹P{¹H} NMR (δ , 121.421 MHz, C₆D₆): -11.87 (s). Found: C, 55.1; H, 8.6; N, 1.9. Calc. for $C_{32}H_{58}ClNSi_2P_2Zr$: C, 54.8; H, 8.3; N, 2.0%.

$Zr(\eta^5-C_5H_5)CH_2SiMe_3[N(SiMe_2CH_2PPr^i_2)_2]$ (8). To a solution of **3** (250 mg, 0.43 mmol) in toluene (10 cm³) was added a solution of Me_3SiCH_2Li (42 mg, 0.45 mmol) in toluene (3 cm³) at room temperature. After stirring for 12 h the solvent was stripped off under reduced pressure, and the resulting solid was extracted with pentane (10 cm³). The filtrate was filtered through a layer of Celite[®] and concentrated (~ 3 cm³) and then cooling this solution at $-40^\circ C$ gave a dark green crystalline product (165 mg, 60%). ESR (toluene): $g = 1.973$; $a(^{91}Zr) = 30.5$ G, 1Zr; $a(^{31}P) = 21.4$ G, 2P; $a(^1H_z) = 9.3$ G, 1H; $a(^1H_x) = 6.2$ G, 1H; $a(^{14}N) = 2.0$ G, 1N; linewidth used for simulation, 2.6 G. μ_{eff} (Evans method) = 1.71 B. M. UV-vis (toluene, 1 cm quartz cell): $\lambda_{max} = 334$ nm, $\epsilon_{max} = 2700$ dm³ mol⁻¹ cm⁻¹; $\lambda = 430$ nm, $\epsilon = 1700$ dm³ mol⁻¹ cm⁻¹. Found: C, 50.7; H, 9.5; N, 2.2. Calc. for $C_{27}H_{60}NP_2Si_3Zr$: C, 50.7; H, 9.5; N, 2.2%.

$Zr(\eta^5-C_5H_5)OPh[N(SiMe_2CH_2PPr^i_2)_2]$ (10). To a solution of **3** (200 mg, 0.34 mmol) in THF (10 cm³) was added a solution of $PhONa$ (40 mg, 0.34 mmol) in THF (5 cm³) at $-10^\circ C$ and stirred for 10 min. The reaction was then warmed to room temperature and stirred for 12 h to give a deep green solution. The solvent was stripped off *in vacuo*, and the resulting solid was extracted with hexanes (10 cm³). The extract was filtered through a layer of Celite[®], concentrated (~ 3 cm³) and cooled at $-40^\circ C$ to give a dark green crystalline product (130 mg, 60%). ESR (toluene): $g = 1.955$; $a(^{31}P) = 18.7$ G, 2P. Found: C, 54.0; H, 8.5; N, 2.1. Calc. for $C_{29}H_{54}NOP_2Si_2Zr$: C, 54.2; H, 8.5; N, 2.2%.

$Zr(\eta^5-C_5H_5)NPh_2[N(SiMe_2CH_2PPr^i_2)_2]$ (11). To a solution of **3** (200 mg, 0.34 mmol) in THF (10 cm³) was added a solution of $NaNPh_2$ (66 mg, 0.34 mmol) in THF (5 cm³) at $-10^\circ C$ and stirred for 10 min. The reaction was then warmed to room temperature and stirred for 12 h to give a deep brown solution. The solvent was stripped off *in vacuo*, and the resulting solid was extracted with hexanes (10 cm³). The extract was filtered through a layer of Celite[®] and stripping off the solvent gave an oil. ESR (toluene): $g = 1.953$; $a(^{31}P) = 11.2$ G, 2P.

$Zr(\eta^5-C_5H_5)PPh_2[N(SiMe_2CH_2PPr^i_2)_2]$ (12). To a solution of **3** (200 mg, 0.34 mmol) in THF (10 cm³) was added a solution of $LiPPh_2$ (66 mg, 0.34 mmol) in THF (5 cm³) at $-10^\circ C$ and stirred for 10 min. The reaction was then warmed to room temperature

and stirred for 12 h to give a deep brown solution. The solvent was stripped off *in vacuo*, and the resulting solid was extracted with hexanes (10 cm³). The extract was filtered through a layer of Celite[®] and stripping off the solvent gave an oil. ESR (toluene): $g = 1.965$; $a(^{31}\text{P}) = 18.6$ G, 2P; $a(^{31}\text{P}) = 29.8$ G.

$\text{Hf}(\eta^5\text{-C}_5\text{H}_5)\text{Cl}_2[\text{N}(\text{SiMe}_2\text{CH}_2\text{PPr}^i_2)_2]$ (**13**). To a solution of $\text{HfCl}_3[\text{N}(\text{SiMe}_2\text{CH}_2\text{PPr}^i_2)_2]$ (6.00 g, 8.89 mmol) in toluene (150 cm³) was added solid $\text{NaCp} \cdot \text{DME}$ (1.736 g, 9.74 mmol) at room temperature. The $\text{NaCp} \cdot \text{DME}$ was added in three portions at 1 h intervals and the resulting mixture was stirred for 12 h. The salt (NaCl) was removed by filtering through Celite[®], the filtrate concentrated to 15 cm³, hexanes were added until the solution turned turbid and cooling at -30°C gave a pale white crystalline material (5.52 g, 88%). ¹H NMR (δ , 300 MHz, C₆D₆): 0.60 [s, 12H, Si(CH₃)₂]; 1.6–0.96 (m, 28H, P[CH(CH₃)₂]₂, SiCH₂P); 2.17 (sept, 4H, P[CH(CH₃)₂]₂, ³J(H—H) = 8.9 Hz); 6.46 (br s ~ 5H, C₅H₅). ³¹P{¹H} NMR (δ , 121.421 MHz, C₆D₆): 20.04 (s). Found: C, 39.4; H, 7.2; N, 1.9. Calc. for C₂₃H₄₉NCl₂P₂Si₂Hf: C, 39.1; H, 7.0; N, 2.0%.

$\text{Hf}(\eta^5\text{-C}_5\text{H}_5)\text{Cl}[\text{N}(\text{SiMe}_2\text{CH}_2\text{PPr}^i_2)_2]$ (**14**). A solution of $\text{Hf}(\eta^5\text{-C}_5\text{H}_5)\text{Cl}_2[\text{N}(\text{SiMe}_2\text{CH}_2\text{PPr}^i_2)_2]$ (2.00 g, 2.83 mmol) in toluene (80 cm³) was transferred into a thick-walled reaction flask containing Na/Hg (100 g of 0.33% amalgam, 14.1 mmol). The flask was then evacuated (3 min) and sealed. Upon stirring the reaction mixture turned deep greenish brown. After 48 h, the reaction mixture was decanted from the amalgam and filtered through a layer of Celite[®]. The amalgam was extracted with 20 cm³ portions of hexanes (total of 60 cm³), until the extracts show no colour. Upon stripping off solvent from the combined filtrate and extracts a dark brown solid was obtained. Pure material was obtained after two recrystallizations from a pentane solution (0.8 g, 47%); after the first recrystallization, the elemental analyses were off by 1–2% in the carbon and the ESR spectrum of the crude brown solid showed the presence of both the zirconium complex **3** and the desired hafnium derivative **14**. During the second recrystallization, some insoluble brown solid was obtained and identified as the dinitrogen complex **1** by ³¹P{¹H} NMR spectroscopy. ESR (toluene): $g = 1.916$. Found: C, 41.5; H, 7.5; N, 2.0. Calc. for C₂₃H₄₉NClP₂Si₂Hf: C, 41.1; H, 7.3; N, 2.1%.

Oxidation reactions

Oxidation reactions with TiCl₃ or PbCl₂ were carried out by adding an excess of solid oxidant (approximately 10 equiv.) to a cooled (approx-

mately -10°C) toluene solution of the zirconium(III) complex. The resulting yellow or orange solution was then decanted, toluene was stripped off, and the residue was extracted with pentane and filtered through a layer of Celite[®].

Oxidation with Ph₂S₂ was carried out by adding a toluene solution of the oxidant (0.5 equiv.) to a solution of the zirconium(III) complex at -78°C . Analytically pure chlorothiolate complex (**15**) was obtained (75%) by recrystallization from Et₂O. The alkylthiolate complexes gave only an oily material and therefore were not analysed.

$\text{Zr}(\eta^5\text{-C}_5\text{H}_5)\text{Cl}(\text{SPh})[\text{N}(\text{SiMe}_2\text{CH}_2\text{PPr}^i_2)_2]$ (**15**). ¹H NMR (δ , 300 MHz, C₆D₆): 0.71 [s, 6H, Si(CH₃)₂]; 0.74 [s, 6H, Si(CH₃)₂]; 0.93–1.15 (m, 24H, P[CH(CH₃)₂]₂); 1.15–1.26 (m, 4H, SiCH₂P); 2.28 (m, 4H, P[CH(CH₃)₂]₂); 6.33 (s, 5H, Cp); 7.05 [t, 1H, *p*-Ph, ³J(H—H) = 7.4 Hz]; 7.24 (m, 2H, *m*-Ph); 7.47 [d, 2H, *o*-Ph, ³J(H—H) = 7.4 Hz]. ³¹P{¹H} NMR (δ , 121.421 MHz, C₆D₆): 13.74 (s). ¹³C{¹H} NMR (δ , 50.324 MHz, C₆D₆): 113.34 (s, Cp). Found: C, 50.1; H, 7.9; N, 1.9. Calc. for C₂₉H₅₄NClSi₃P₂SZr: C, 50.2; H, 7.8; N, 2.0%.

$\text{Zr}(\eta^5\text{-C}_5\text{H}_5)\text{ClEt}[\text{N}(\text{SiMe}_2\text{CH}_2\text{PPr}^i_2)_2]$. Complex **6** was oxidized with PbCl₂. ¹H NMR (δ , 300 MHz, C₆D₆): 0.40 [br s, 6H, Si(CH₃)₂, $\Delta\nu_{1,2} = 40$ Hz]; 0.55 [s, 6H, Si(CH₃)₂, $\Delta\nu_{1,2} = 40$ Hz]; 0.75–0.90 (br, 6H, SiCH₂P and CH₂CH₃); 0.95–1.10 (m, 24H, P[CH(CH₃)₂]₂); 1.78 (br m, 4H, P[CH(CH₃)₂]₂); 1.78 [t, 3H, CH₂CH₃, ³J(H—H) = 7.6 Hz]; 6.33 (s, Cp, 5H). ³¹P{¹H} NMR (δ , 121.421 MHz, C₆D₆): -0.5 (br, s, $\Delta\nu_{1,2} = 370$ Hz); 8.0 (br s, $\Delta\nu_{1,2} = 370$ Hz). Found: C, 48.3; H, 8.6; N, 2.2. Calc. for C₂₅H₅₄ClNSi₃P₂SZr: C, 48.9; H, 8.9; N, 2.3%.

$\text{Zr}(\eta^5\text{-C}_5\text{H}_5)\text{Cl}(\text{CH}_2\text{Ph})[\text{N}(\text{SiMe}_2\text{CH}_2\text{PPr}^i_2)_2]$. Complex **7** was oxidized with TiCl₃. ¹H NMR (δ , 300 MHz, C₆D₆): 0.40 [br s, 6H, Si(CH₃)₂]; 0.50 [s, 6H, Si(CH₃)₂]; 0.70 (br, 4H, SiCH₂P); 0.90–1.0 (m, 24H, P[CH(CH₃)₂]₂); 1.70 (br m, 4H, P[CH(CH₃)₂]₂); 2.68 [d, 1H, CH₂Ph, ²J(H—H) = 11 Hz]; 2.98 [d, 1H, CH₂Ph, ²J(H—H) = 11 Hz]; 6.20 (s, Cp, 5H). ³¹P{¹H} NMR (δ , 121.421 MHz, C₆D₆): -0.5 (br s, $\Delta\nu_{1,2} = 370$ Hz); 8.0 (br s, $\Delta\nu_{1,2} = 370$ Hz).

$\text{Zr}(\eta^5\text{-C}_5\text{H}_5)\text{CH}_2\text{SiMe}_3(\text{SPh})[\text{N}(\text{SiMe}_2\text{CH}_2\text{PPr}^i_2)_2]$. Spectra were recorded within 2 h after the reaction. ¹H NMR (δ , 300 MHz, C₆D₆): 0.32 [s, 9H, CH₂Si(CH₃)₃]; 0.42 [s, 6H, Si(CH₃)₂]; 0.52 [s, 6H, Si(CH₃)₄]; 0.87 (m, 4H, SiCH₂P); 0.98–1.12 (m, 26H, P[CH(CH₃)₂]₂ and CH₂Si(CH₃)₃); 1.80 (m, 4H, P[CH(CH₃)₂]₂); 6.40 (s, 5H, Cp); 6.98 [t, 1H, *p*-Ph, ³J(H—H) = 7.3 Hz]; 7.18 (m, 2H, *m*-Ph); 7.83 [d, 2H, *o*-Ph, ³J(H—H) = 7.4 Hz]. ³¹P{¹H} NMR (δ , 121.421 MHz, C₆D₆): 2.50 (br s).

Complicated spectra were obtained after 7 days. ¹H NMR (δ , 300 MHz, C₆D₆): 6.08 (s, 5H, Cp);

Table 6. Summary of data collection and structure refinement details for $Zr(\eta^5-C_5H_5)C_6H_5[N(SiMe_2CH_2PPr^i_2)_2]$ (**4**) and $Zr(\eta^5-C_5H_5)CH_2SiMe_3[N(SiMe_2CH_2PPr^i_2)_2]$ (**8**)

	$Zr(\eta^5-C_5H_5)C_6H_5$ $[N(SiMe_2CH_2PPr^i_2)_2]$ (4)	$Zr(\eta^5-C_5H_5)CH_2SiMe_3$ $[N(SiMe_2CH_2PPr^i_2)_2]$ (8)
Formula	ZrSi ₂ P ₂ NC ₂₉ H ₅₄	ZrSi ₃ P ₂ NC ₂₇ H ₆₀
f_w	626.08	636.21
Crystal system	Triclinic	Monoclinic
a (Å)	9.0970(10)	10.0813(19)
b (Å)	10.512(3)	17.7883(18)
c (Å)	19.079(5)	20.414(4)
α (°)	90.90(3)	
β (°)	95.890(10)	100.243(22)
γ (°)	107.390(20)	
V (Å ³)	1729.8(7)	3602.5(10)
Space group	$P\bar{1}$	$P2_1/c$
Z	2	4
d_{calc} (mg m ⁻³)	1.202	1.17
$F(000)$	660	1364
μ (mm ⁻¹)	0.49	0.50
R_F	0.036	0.039
R_w	0.038	0.043
Gof	2.67	4.37

6.28 (s, 5H, Cp). ³¹P{¹H} NMR (δ , 121.421 MHz, C₆D₆): -1.9 (s), -2.2 (s), 18.6 (s), 18.8 (s).

$Zr(\eta^5-C_5H_5)CH_2CH_3(SPh)[N(SiMe_2CH_2PPr^i_2)_2]$. Spectra were recorded within 2 h after the reaction. ¹H NMR (δ , 300 MHz, C₆D₆): 0.45 [br s, 6H, Si(CH₃)₂, $\Delta v_{1,2}$ = 35 Hz]; 0.68 [br s, 6H, Si(CH₃)₂, $\Delta v_{1,2}$ = 35 Hz]; 0.85–0.90 (br m, 6H, SiCH₂P and CH₂CH₃); 0.95–1.15 (m, 24H, P[CH(CH₃)₂]₂); 1.75 (m, 4H, P[CH(CH₃)₂]₂); 1.81 [t, 3H, CH₂CH₃, ³J(H–H) = 6.7 Hz]; 6.13 (s, 5H, Cp); 7.00 [t, 1H, *p*-Ph, ³J(H–H) = 7.0 Hz]; 7.18 (m, 2H, *m*-Ph); 7.70 [d, 2H, *o*-Ph, ³J(H–H) = 7.0 Hz]. ³¹P{¹H} NMR (δ , 121.421 MHz, C₆D₆): -1.0 (br s, $\Delta v_{1,2}$ = 250 Hz); 11.0 (br s, $\Delta v_{1,2}$ = 250 Hz).

Complex spectra were obtained after 7 days. ¹H NMR (δ , 300 MHz, C₆D₆): 6.05 (s, 5H, Cp); 6.24 (s, 5H, Cp). ³¹P{¹H} NMR (δ , 121.421 MHz, C₆D₆): -1.8 (s), -2.1 (s), 18.6 (s), 18.8 (s).

X-ray Crystallography

Crystals were mounted in thin-walled glass capillaries and optically centred in the X-ray beam of an Enraf–Nonius CAD-4 diffractometer. Unit-cell dimensions were determined via least squares refinement of the setting angles of 24 high angle reflections and intensity data were collected using the ω -2 θ scan mode. Data were corrected for Lorentz, polarization and absorption effects but not for extinction. Pertinent data collection and structure refinement parameters are presented in Table 6. All structures were solved using direct

methods. All non-hydrogen atoms were refined with anisotropic thermal parameters. Methyl and methylene hydrogen atoms were located by inspection of difference Fourier maps and fixed, temperature factors being based upon the carbon to which they are bonded. For compound **8**, three methyl carbon atoms [C(8A), C(8B), C(8C)] were refined with the site occupancy as a variable, affording occupancy factors of 0.8691, 1.2318, 0.7825 for C(8A), C(8B) and C(8C), respectively. The corresponding hydrogen atoms were therefore not locateable. A weighting scheme based upon counting statistics was used with the weight modifier k in kF_o^2 being determined via evaluation of variation in the standard reflections that were collected during the course of data collection. Neutral atom scattering parameters were taken from *International Tables for X-ray Crystallography*.⁷⁶ Values of R_F and R_w are given by $R_F = \Sigma(F_o - F_c) / \Sigma F_o$ and $R_w = \{\Sigma[w(F_o - F_c)^2 / \Sigma(wF_o^2)]\}^{1/2}$. All crystallographic calculations were conducted with the PC version of the NRCVAX program package⁷⁷ locally implemented on an IBM compatible 80486 computer.

Acknowledgement—Financial support was provided by NSERC of Canada in the form of operating grants to M. D. F. and M. J. Z.

REFERENCES

1. J. P. Collman, L. S. Hegedus, J. R. Norton and R. G.

- Finke, *Principles and Applications of Organotransition Metal Chemistry*. University Science Books, Mill Valley, CA. (1987).
2. F. A. Cotton and G. Wilkinson, *Advanced Inorganic Chemistry*. Wiley, Toronto (1980).
 3. N. N. Greenwood and A. Earnshaw, *Chemistry of the Elements*. Pergamon Press, Oxford (1984).
 4. D. J. Cardin, M. F. Lappert and C. L. Raston, *Chemistry of Organo-Zirconium and Hafnium Compounds*. Ellis Horwood Limited, Toronto (1986).
 5. M. F. Lappert and C. L. Raston, *J. Chem. Soc., Chem. Commun.* 1980, 1284.
 6. M. F. Lappert, C. J. Pickett, P. I. Riley and P. I. W. Yarrow, *J. Chem. Soc., Dalton Trans.* 1981, 805.
 7. C. S. Bajgur, W. Tikkanen and J. L. Petersen, *Inorg. Chem.* 1985, **24**, 2539.
 8. R. Choukroun, F. Dahan, A. M. Larssonneur, E. Samuel, J. Peterson, P. Meunier and C. Sornay, *Organometallics* 1991, **10**, 374.
 9. D. G. Dick and D. W. Stephan, *Can. J. Chem.* 1991, **69**, 1146.
 10. Y. Wielstra, S. Gambarotta and A. Meetsma, *Organometallics* 1989, **8**, 2948.
 11. Y. Wielstra, S. Gambarotta, A. Meetsma and J. L. d. Boer, *Organometallics* 1989, **8**, 250.
 12. M. Y. Chiang, S. Gambarotta and F. v. Boihuis, *Organometallics* 1988, **7**, 1864.
 13. P. B. Hitchcock, M. F. Lappert, G. A. Lawless, H. Olivier and E. J. Rayn, *J. Chem. Soc., Chem. Commun.* 1992, 474.
 14. K. I. Gell, T. V. Harris and J. Schwartz, *Inorg. Chem.* 1981, **20**, 481.
 15. T. V. Ashworth, T. C. Agreda, E. Herdtweck and W. A. Herrmann, *Angew. Chem., Int. Edn Engl.* 1986, **25**, 289.
 16. S. Gambarotta and M. Y. Chiang, *Organometallics* 1987, **6**, 897.
 17. T. Cuenca, W. A. Herrmann and T. V. Ashworth, *Organometallics* 1986, **5**, 2514.
 18. J. H. Wengrovius, R. R. Schrock and C. S. Day, *Inorg. Chem.* 1981, **20**, 1844.
 19. J. H. Wengrovius and R. R. Schrock, *J. Organomet. Chem.* 1981, **205**, 319.
 20. F. A. Cotton, M. P. Diebold and P. A. Kibala, *Inorg. Chem.* 1988, **27**, 799.
 21. F. A. Cotton, M. Shang and W. A. Wojtczak, *Inorg. Chem.* 1991, **30**, 3670.
 22. G. Erker, W. Fromberg, R. Mynott, B. Gabor and C. Kruger, *Angew. Chem., Int. Edn Engl.* 1986, **25**, 463.
 23. J. D. Cohen, M. Mylvaganam, M. D. Fryzuk and T. M. Loehr, *J. Am. Chem. Soc.* 1994, **116**, 9529.
 24. M. D. Fryzuk, T. S. Haddad, M. Mylvaganam, D. H. McConville and S. J. Rettig, *J. Am. Chem. Soc.* 1993, **115**, 2782.
 25. M. D. Fryzuk, M. Mylvaganam, M. J. Zaworotko and L. R. MacGillivray, *J. Am. Chem. Soc.* 1993, **115**, 10,360.
 26. G. W. A. Fowles, B. J. Russ and G. R. Willy, *CC* 1967, 646.
 27. G. W. A. Fowles and G. R. Willey, *J. Chem. Soc. (A)* 1968, 1435.
 28. E. N. Larsen and T. E. Hehzler, *Inorg. Chem.* 1974, **13**, 581.
 29. D. Nicholls and T. A. Ryan, *Inorg. Chim. Acta* 1977, **21**, L17.
 30. D. M. Hoffman and S. Lee, *Inorg. Chem.* 1992, **31**, 2675.
 31. M. Bénard and M.-M. Rohmer, *J. Am. Chem. Soc.* 1992, **114**, 4785.
 32. S. Gambarotta, Y. Wielstra, A. L. Spek and W. J. J. Smeets, *Organometallics* 1990, **9**, 2142.
 33. G. P. Pez, C. F. Putnik, S. L. Suib and G. D. Stucky, *J. Am. Chem. Soc.* 1979, **101**, 6933.
 34. Y. Wielstra, S. Gambarotta, A. L. Spek and W. J. J. Smeets, *Organometallics* 1990, **9**, 2142.
 35. G. M. Williams and J. Schwartz, *J. Am. Chem. Soc.* 1982, **104**, 1122.
 36. J. M. Atkinson, P. B. Brindley, A. G. Davis and J. A. A. Hawari, *J. Organomet. Chem.* 1984, **264**, 253.
 37. C. S. Bajgur, S. B. Jones and J. L. Petersen, *Organometallics* 1985, **4**, 1929.
 38. R. T. Baker, J. F. Whitney and S. S. Wreford, *Organometallics* 1983, **2**, 1049.
 39. C. Blandy, S. A. Locke, S. J. Young and N. E. Schore, *J. Am. Chem. Soc.* 1988, **110**, 7540.
 40. R. Choukroun and D. Gervais, *J. Chem. Soc., Chem. Commun.* 1985, 224.
 41. R. Choukroun, M. Basso-Bert and D. Gervais, *J. Chem. Soc., Chem. Commun.* 1986, 1317.
 42. R. Choukroun, D. Gervais and Y. Raoult, *Polyhedron* 1989, **8**, 1758.
 43. R. Choukroun, F. Dahan, D. Gervais and C. Rifai, *Organometallics* 1990, **9**, 1982.
 44. M. Etienne, R. Choukroun and D. Gervais, *J. Chem. Soc., Dalton Trans.* 1984, 915.
 45. M. J. S. Gynane, J. Jeffery and M. F. Lappert, *J. Chem. Soc., Chem. Commun.* 1978, 34.
 46. A. Hudson, M. F. Lappert and R. Pichon, *J. Chem. Soc., Chem. Commun.* 1983, 374.
 47. Y. Raoult, R. Choukroun and C. Blandy, *Organometallics* 1992, **11**, 2443.
 48. E. Samuel, *Inorg. Chem.* 1983, **22**, 2967.
 49. N. E. Schore, S. J. Young, M. Olmstead and P. Hofmann, *Organometallics* 1983, **2**, 1769.
 50. J. Blenkins, P. Bruin and J. H. Teuben, *J. Organomet. Chem.* 1985, **297**, 61.
 51. R. D. Rogers and J. H. Teuben, *J. Organomet. Chem.* 1989, **359**, 41.
 52. D. Gourier, E. Samuel and J. H. Teuben, *Inorg. Chem.* 1989, **28**, 4663.
 53. I. F. Urazowski, V. I. Ponomaryev, I. E. Nifantev and D. A. Lemenovskii, *J. Organomet. Chem.* 1989, **368**, 287.
 54. H. Brand and J. Arnold, *Angew. Chem., Int. Edn Engl.* 1994, **33**, 95.
 55. M. F. Lappert, P. I. Riley and P. I. W. Yarrow, *J. Chem. Soc., Chem. Commun.* 1979, 305.
 56. P. M. Morse, S. R. Wilson and G. S. Girolami, *Inorg. Chem.* 1990, **29**, 3200.
 57. B. N. Figgis and J. Lewis, *Prog. Inorg. Chem.* 1964, **6**, 37.
 58. T. V. Lubben, P. T. Wolczanski and G. D. van Duyne, *Organometallics* 1984, **3**, 977.

59. R. W. Fessenden and R. H. Schuler, *J. Chem. Phys.* 1963, **39**, 2147.
60. R. J. Fitzgerald and R. S. Drago, *J. Am. Chem. Soc.* 1968, **90**, 2523.
61. M. Brookhart and M. L. H. Green, *J. Organomet. Chem.* 1983, **250**, 395.
62. M. Brookhart, M. L. H. Green and L. Wong, *Prog. Inorg. Chem.* 1988, **36**, 1.
63. P. Legzdins, R. H. Jones, E. C. Phillips, V. C. Yee, J. Trotter and F. W. B. Einstein, *Organometallics* 1991, **10**, 986.
64. M. D. Fryzuk, A. Carter and A. Westerhaus, *Inorg. Chem.* 1985, **24**, 642.
65. M. D. Fryzuk, S. J. Rettig, A. Westerhaus and H. G. Williams, *Inorg. Chem.* 1985, **24**, 4316.
66. M. D. Fryzuk, T. S. Haddad and S. J. Rettig, *Organometallics* 1988, **7**, 1224.
67. M. D. Fryzuk, T. S. Haddad and S. J. Rettig, *Organometallics* 1989, **8**, 1723.
68. G. A. Luinstra, J. Vogelzang and J. H. Teuben, *Organometallics* 1992, **11**, 2273.
69. W. E. Piers, L. S. Koch, D. S. Ridge, L. R. MacGillivray and M. J. Zaworotko, *Organometallics* 1992, **11**, 3148.
70. M. Schlosser and V. Ladenberger, *J. Organomet. Chem.* 1967, **8**, 193.
71. D. Bryce-Smith and E. E. Turnrt, *J. Chem. Soc.* 1953, 861.
72. M. Schlosser and J. Hartmann, *Angew. Chem., Int. Edn Engl.* 1973, **12**, 508.
73. R. R. Schrock and J. D. Fellmann, *J. Am. Chem. Soc.* 1978, **100**, 3359.
74. J. C. Smart and C. J. Curtis, *Inorg. Chem.* 1977, **16**, 1788.
75. R. R. Schrock, *J. Organomet. Chem.* 1976, **122**, 209.
76. *International Tables for X-ray Crystallography*, Vol. IV. Kynoch Press, Birmingham (1974).
77. E. J. Gabe, Y. Le Page, J.-P. Charland, F. L. Lee and P. S. White, *J. Appl. Cryst.* 1989, **22**, 384.